POS1-45

# The $SAR_{10g}$ estimation in human head Phantom with optical fibre thermometer

Toshiya Sato Yoshinobu OKANO
Musashi Institute of Technology
1-28-1 Tamadutumi, Setagaya-ku, Tokyo 158-0087 Japan
E-mail t-satou@rw.ec.musashi-tech.ac.jp

## 1. Introduction

Recently, mobile communication equipments are necessary and indispensable. The electromagnetic energy from mobile device gives thermal effect to the human body. This effect is evaluated with Specific Absorption Rate (SAR). In present, most practicable SAR evaluation method is electric field probe scanning method. The SAR evaluation by a physically different approach is necessary. Hence, the thermal SAR evaluation method is proposed. The actual experiment is performed to estimate the SAR in semi-solid phantom exposed to microwave source by using the thermometer installed in phantom. The optical fibre thermometer is used to avoid the electromagnetic field disturbance around the thermometer. If thermal diffusion is negligibly small, the SAR is given by

$$SAR = \frac{C \cdot \Delta T}{\Delta t} \quad [W / kg]$$

where , C[J/kg K] is the specific heat of the phantom material, $\Delta$T[K] is the temperature rise measured with thermometer, and $\Delta$t [s] is the exposure duration. If the average temperature rise in 10g-mass can be measured, 10g-mass averaged SAR is obtained by expression (1).

In this paper, thermal evaluation method for the 10g-mass averaged SAR($SAR_{10g}$) is explained.

## 2. $SAR_{10g}$ estimation system

### 2.1 Concept of the thermal SAR evaluation method.

The multiple temperature rise measurement points are necessary to evaluate $SAR_{10g}$. The measurement points are showed in Fig.1.

In phantom material that density is near to 1000kg/m$^3$, a side length of 10g-mass cube is about 21.5mm. When the temperature measurement point is arranged at 5mm intervals in the cube to contain 10g-mass (25mm x 25mm x 25mm), the numbers of measurement points are 125 (see Fig.1). However, the temperature measurement point is omitted from 125 to 45 if there is symmetry in irradiation source (see Fig. 2 (b)). Additionally, measurement point is omitted from 45 to 13 when it can be considered that the temperature inclination to the direction of the electromagnetic field penetration is approximately uniform (see Fig. 2 (c)). In that case, if the temperature distribution from Layer#1 to Layer#5 is measured only by one row, the temperature distribution of other rows can be presumed.

Table 1 shows analytical results of SAR attenuation rate from Layer#1 to Layer#5 with a 2 GHz half wavelength dipole antenna as irradiation source. If thermal diffusion is negligibly, SAR and the temperature rise are proportional. Accordingly, it is predictable that temperature inclination for electromagnetic field penetration depth is almost uniform from Table 1.

SAR attenuation rate on Layer#1 based on the SAR value at the nearest point of 2 GHz dipole antenna's feed point (A1-point) is shown in Table 2. Table 2(a) shows the SAR attenuation rate in a parallel direction to the antenna. Table 2(b) is orthogonal SAR attenuation rate to the antenna. The results in Table 2 shows that primary data on Layer#1 exists in five points of A1, B1, C1, A2, and A3. It is predicted that the measurement point on Layer#1 can be decreased from 9 to 5 (see Fig. 2 (d)). Actually, A1, B1, C1, B2, and A3 are chosen as a measurement point for the convenience of the temperature sensor arrangement. After all, it is thought that the measurement point can be omitted in nine points in all. Table 1 and 2 are analytical results by finite-difference time-domain (FDTD) method.

ISBN: 978-4-88552-223-9 C3055©IEICE

Each primary and subsidiary measurement points are assumed to indicate average temperature rise in a sample cube (5mm x 5mm x 5mm =125mm$^3$ cube). Therefore, the weight coefficient is multiplied by those average temperature rise value, and it is added each other. When the weight coefficient corresponds to the volume ratio that each sample cube occupies in 10g-mass, the amount of temperature rise value in sample cube reaches the average temperature rise in 10g-mass. The part of sample cube that protrude from 10g-mass is pared off. The $SAR_{10g}$ is calculated by substituting average temperature rise in 10g-mass for expression (2).

$$SAR = \frac{C \cdot \Delta T_{10g}}{\Delta t} \qquad [W/kg]$$

where, ΔT10g [K] is the average temperature rise in 10g-mass.

### 2.2 Phantom material

The shape of the semi-solid phantom for the measurement is set to width = 200 mm, depth = 100 mm, and height = 200 mm (see Fig.1). The phantom is homogeneous structure and electric equivalent to the body tissue. Three kinds of semi-solid phantom recipes were prepared corresponding to the frequency bands (for 2 to 2.5GHz, 2.5 to 3.5GHz and 3.5 to 5GHz band). The material composition ratios of the semi-solid phantom are listed in Table 3. The dielectric properties and material properties of the phantom are listed in Table 4.

Dielectric properties of manufactured brain equivalent phantom is shown in Fig. 1 with the brain tisisue data at the FCC (Federal Communications Commission) presentation [1]. The error bars are set within the ± 5% range. The relative permittivity and conductivity aere measured with 85070C permittivity probe manufactured by Agilent Technologies Ltd. The date of the density and specific heat is due to the measurement of Agne technical center Ltd.

### 2.3 Measurement system

The electromagnetic wave is exposed to the phantom for a short time, and, as a result, the temperature rise caused in the phantom is measured with an optical fibre thermometer. The electromagnetic source uses a half-wavelength dipole antenna at 2.0, 2.4, 3.0, 3.5, 4.0, 4.5 and 5.0 GHz. The distance between the antenna and the phantom is 15mm. The irradiation power is set to larger value (= 20 W) than an actual cellular phone output [2]. The purpose of emphasizing irradiation power is to expand resolution and a dynamic range in optical fibre thermometer. The exposure duration is set to 30 seconds.

When the microwave is irradiated to the phantom, temperature rise in phantom is influenced by thermal diffusion. The effect of thermal transfer in thermal diffusion has been cancelled by multiplying correction coefficient (= 1.1) by the temperature measurement value on Layer#1 [2].

## 3. Result and Discussion

Fig.4 shows the comparison between the calculated results by FDTD method and the measured results by the thermal $SAR_{10g}$ evaluation method. Calculated and measured SAR are compared at about 500MHz intervals in 2 to 5GHz frequency band. In the 2 to 4GHz region, calculated SAR datas are higher than measured one. However, in the 4.5 to 5GHz region, calculated SAR datas are lower than measured one. The difference between thermal method SAR data and numerical calculated data are 6% or less.

## 4. Conclusion

In this paper, the establishment of the thermal $SAR_{10g}$ estimation method with the optical fibre thermometer was tried. Thermal method can estimate $SAR_{10g}$ with the difference of about 6% to numerical calculated data. Therefore, the validity of this method was proven.

## References

[1] http://www.fcc.gov/fcc-bin/dielec.sh
[2] Y. Okano, Y. Sugama, M.Abe, “The SAR evaluation method with optical fiber thermometer,” EMC Zurich 2005, pp.161-166, Feb.2005.

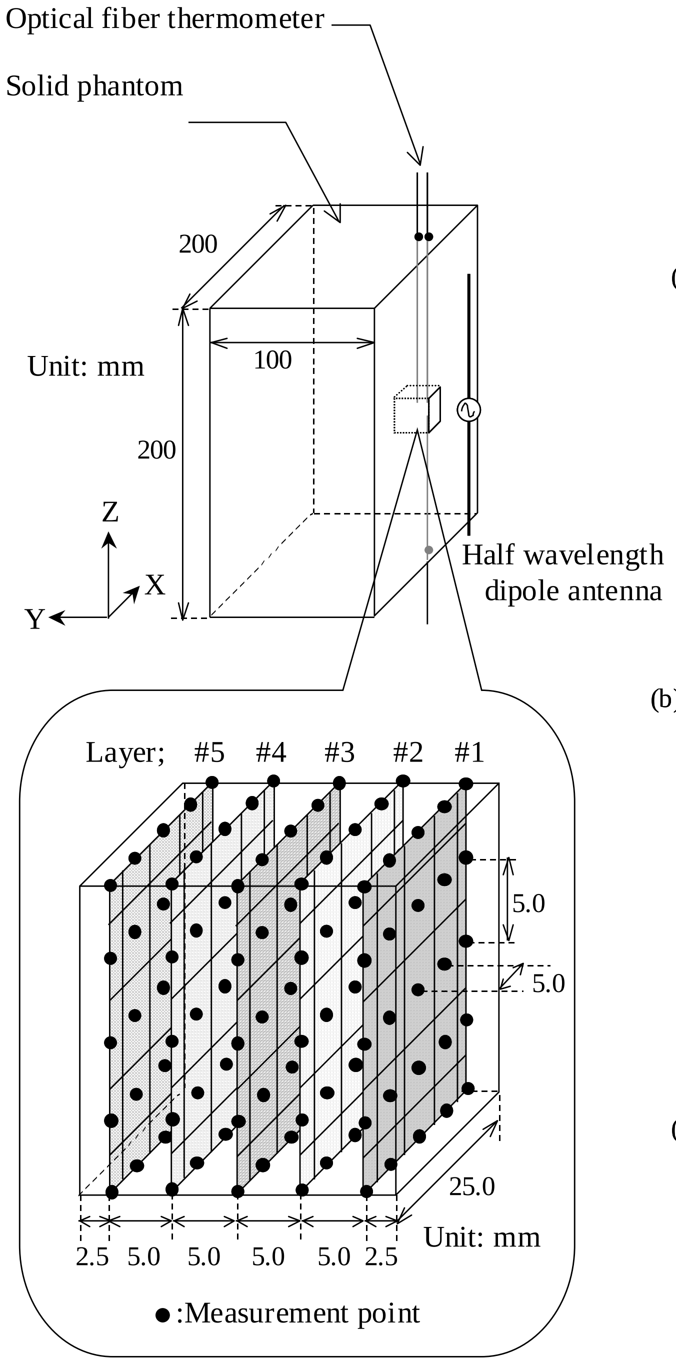


Fig.1 Concept chart of the thermal SAR evaluation method and location of the optical fibre thermometer.

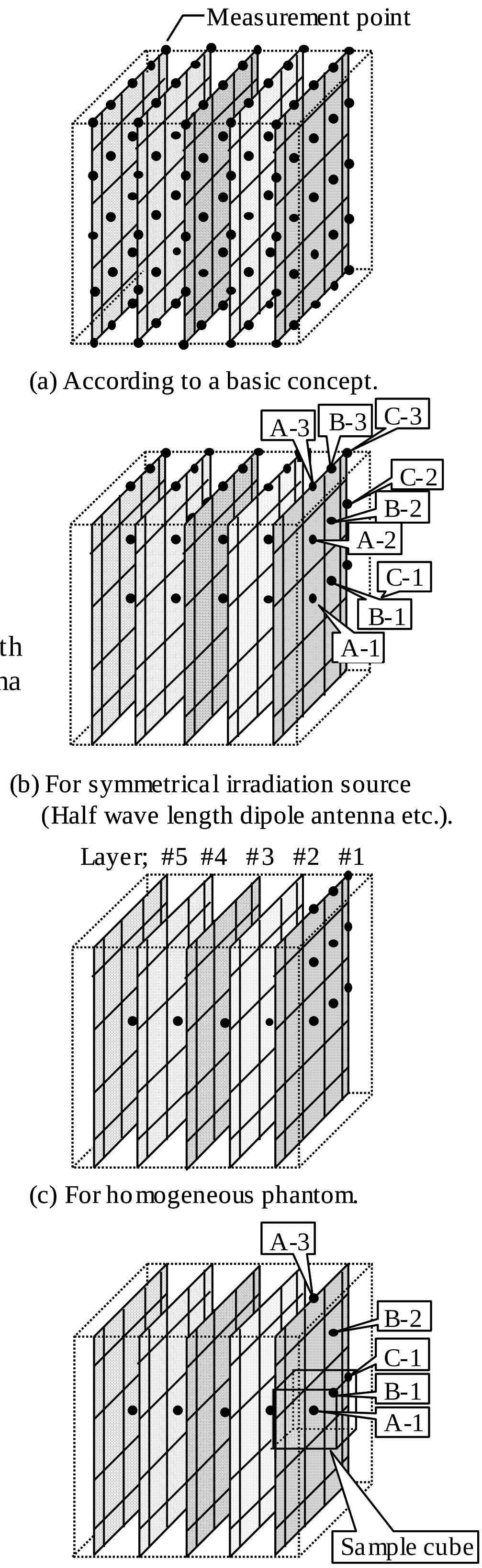


(a) According to a basic concept.

(b) For symmetrical irradiation source (Half wave length dipole antenna etc.).

(c) For homogeneous phantom.

(d) For the case that temperature rise value distribution in Layer#1 is symmetric.

Fig.2 Omission procedure of temperature measurement point

Table.1
SAR attenuation rate transition to electromagnetic field penetration direction at 2GHz.

| | SAR attenuation rate | | | | | | | | |
|---|---|---|---|---|---|---|---|---|---|
| Depth [mm] | A1 | A2 | A3 | B1 | B2 | B3 | C1 | C2 | C3 |
| 2.5 | 1.00 | 1.00 | 1.00 | 1.00 | 1.00 | 1.00 | 1.00 | 1.00 | 1.00 |
| 7.5 | 0.62 | 0.62 | 0.62 | 0.64 | 0.64 | 0.64 | 0.67 | 0.67 | 0.67 |
| 12.5 | 0.39 | 0.39 | 0.39 | 0.41 | 0.41 | 0.41 | 0.45 | 0.45 | 0.45 |
| 17.5 | 0.25 | 0.25 | 0.25 | 0.26 | 0.26 | 0.26 | 0.30 | 0.30 | 0.30 |
| 22.5 | 0.16 | 0.17 | 0.16 | 0.17 | 0.19 | 0.17 | 0.20 | 0.20 | 0.20 |

Table.2
SAR attenuation rate transition to electromagnetic field penetration direction at 2GHz .

(a) SAR attenuation rate in a parallel to the antenna.

| Later #1 | SAR attenuation rate |
|---|---|
| A2/A1 | 0.97 |
| A3/A1 | 0.87 |
| B2/B1 | 0.97 |
| B3/B1 | 0.87 |
| C2/C1 | 0.97 |
| C3/C1 | 0.87 |

(b) SAR attenuation rate in a orthogonal to the antenna

| Later #1 | SAR attenuation rate |
|---|---|
| B1/A1 | 0.90 |
| C1/A1 | 0.64 |
| B2/A2 | 0.90 |
| C2/A2 | 0.64 |
| B3/A3 | 0.90 |
| C3/A3 | 0.64 |

Table.3
The material composition ratio of the brain-equivalent solid phantom for exposure.

| Material | Weight ratio [%] | | |
|---|---|---|---|
| | 2-2.4GHz | 3-3.5GHz | 4-5GHz |
| Silicon emulsion | 46.5 | 58.0 | 57.0 |
| Deionized water | 27.6 | 26.7 | 33.7 |
| Glycerin | 20.9 | 12.0 | 4.0 |
| Ager | 4.7 | 3.0 | 5.0 |
| Sodium benzoato | 0.3 | 0.3 | 0.3 |

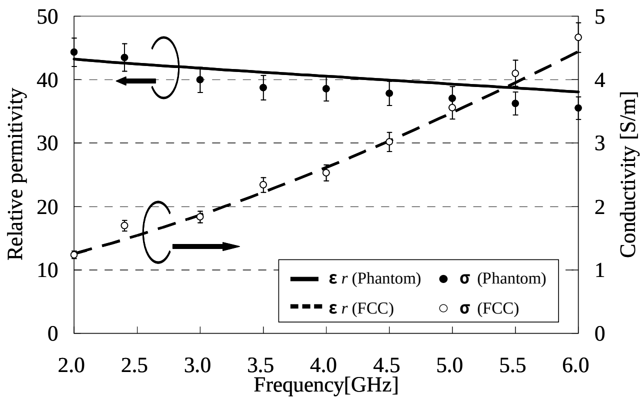


Fig.3 The comparison between the semi-solid phantom's dielectric properties and FCC's one.

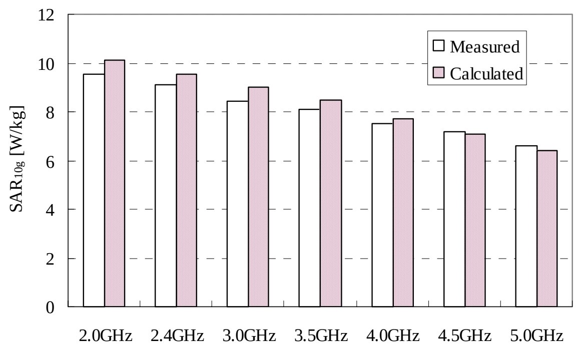


Fig.4 Comparison between numerical, thermal method